

Absolute Cross Sections for the $^{27}\text{Al}(p,3pn)^{24}\text{Na}$
Reaction at 28 and 0.8 GeV.

J. B. Cumming, V. Agoritsas*, and R. Witkover

Brookhaven National Laboratory

Upton, N.Y. 11973

Absolute cross sections for the $^{27}\text{Al}(p,3pn)^{24}\text{Na}$ reaction have been determined to be 7.92 ± 0.18 mb at 28 GeV and 10.94 ± 0.24 mb at 0.8 GeV. In this work, proton beam intensities in the AGS fast external beam were measured with current transformer and integrator systems which were calibrated electrically. The ^{24}Na induced in aluminum foils was assayed by comparing the intensity of its 1368-keV gamma ray with that of the 1332-keV line from calibrated ^{60}Co standards.

*Present address, CERN PS Division
1211 Geneva 23, Switzerland

Introduction

At the present time, the cross section scale for the great majority of nuclear reaction studies at GeV energies is dependent on a few absolute values for the $^{12}\text{C}(p,pn)^{11}\text{C}$ reaction.¹⁻⁶ Choice of this reaction as the primary standard has been determined in large measure by the need to count individual protons, e.g. by emulsion or counter telescope techniques, for the fluence measurements. Absolute beam current determination with a Faraday cup, a procedure widely used at lower energies, has not been employed at energies above 0.8 GeV.⁷ The short, 20.4-min half life of ^{11}C , loss of gases containing ^{11}C from thin targets,^{8,9} foil nonuniformities, and thermal decomposition of plastic in high intensity beams are all disadvantages for the use of the $^{12}\text{C}(p,pn)^{11}\text{C}$ reaction in many situations. Accordingly, secondary standards, particularly the $^{27}\text{Al}(p,3pn)^{24}\text{Na}$ reaction are used frequently to monitor proton beams.¹

In addition to its use in nuclear reaction studies, foil activation has been employed at high-energy accelerators for beam diagnostic and intensity measurements. Foil activation is linear over a wide intensity range and is insensitive to fast intensity variations, i.e., fine structure of beam pulses. It is, of course, free of the effects of surface changes which may influence secondary emission chambers¹⁰. If a foil target is replaced by a wire grid, beam density distributions can be measured with high spatial

resolution. When correctly applied, such data can give accurate emittances.¹¹ A significant disadvantage is the fact that activation is an off-line technique; results only become available after sample assay, typically hours or more after an irradiation.

The $^{12}\text{C}(p,pn)^{11}\text{C}$ cross section previously measured at the AGS full energy (28 GeV) is 25.9 ± 1.2 mb.¹² The $^{27}\text{Al}(p,3pn)^{24}\text{Na}$ secondary monitor cross section is determined from this value and the experimental ratio¹³ $^{27}\text{Al}(p,3pn)^{24}\text{Na}/^{12}\text{C}(p,pn)^{11}\text{C}$ of 0.322 ± 0.009 to be 8.34 ± 0.45 mb. However, a review¹ which considered this value in context with those at lower energies, recommended use of 8.6 ± 0.6 mb for the secondary standard at energies above 10 GeV.

With increases in intensity and the extraction of a fast external beam (FEB) from the AGS,¹⁴ it became possible once more to make reliable electrical measurements of particle fluxes, in this case, not with a Faraday cup, but by determining the charge induced by passing the beam pulses through a transformer as a single turn primary winding. The present paper describes measurements over a three year period which utilized this technique in a variety of experimental conditions to determine directly a precise cross section for the $^{27}\text{Al}(p,3pn)^{24}\text{Na}$ reaction at 28 GeV as an independent check of the cross section scales set previously. Measurements were also performed in an 0.81-GeV beam which had been extracted from the AGS for other experiments.¹⁵ These permit an overlap between the high energy

results and those in the lower energy region which had been performed using different techniques.

The Fast External Beam

The FEB is extracted from the AGS by a shaving system which has been described in detail elsewhere.¹⁴ In brief, a sudden perturbation of the orbit deflects the twelve circulating proton bunches through two thin septum magnets. These, in turn, further deflect the protons into the external beam line (U-line). Each pulse train thus consists of twelve ~20-nsec wide bunches with ~200 nsec separations. The acceleration cycle time is normally 1.6 sec. Extraction efficiencies of >95% are routine for intensities up to 10^{13} protons per pulse in agreement with theoretical predictions.

Protons travel in the U line for 244 m from the ejection section in a 10 cm diameter vacuum pipe, then emerge through a 105-mg/cm² aluminum window, and proceed an additional 4.6 m through air before interacting in a meson production target. A 4.25° bend using conventional dipoles at the 12-m position, and an 8° bend using superconducting dipoles at the 88-m mark set the beam line direction. An array of quadrupoles and steering dipoles provide focusing and positioning capability. A beam loss monitor system consisting of ion chambers adjacent to the U-line allows fine tuning of the components for optimum transmission from the accelerator to the

target. Transport efficiencies of >96% are normal, and values often approach 100%. Several beam current transformers permit measurement of the beam intensities at locations along the line. When calibrated as described below, these devices provided the absolute proton fluences for the cross section measurements.

Targets and Irradiation Procedures

Target stacks were irradiated with 28-GeV protons at two positions in the FEB line. Most experiments were performed with targets in air in the region from 3- to 33-cm downstream of the 105-mg/cm² foil window (designated location U-801¹⁶). Toward the end of the present work, some cross sections were measured with the foils in vacuum in an instrument box at the 51-m position (location U-167). At both positions the full energy beam was ~1 cm in diameter (FWHM). Irradiations at 0.81 GeV were performed only in the instrument box and the spot size was 2-3 times larger than at 28 GeV.

A variety of target configurations were used. Their thickness varied from 30 to 152 mg/cm². The standard target assembly consisted of a central 20-mg/cm² high-purity Al foil guarded on each side by 5-mg/cm² Al, and supported over a ~10-cm hole in a cardboard frame. The guard foils were sufficiently thick to compensate for ²⁴Na recoil losses from the central foil.¹⁷ Multiple central foils, either 20 mg/cm² or 7 mg/cm² thick, were used in several experiments to check

foil uniformity, which was found to be very good. Targets for early experiments contained polyethylene foils to measure the $^{27}\text{Al}(p,3pn)$ $^{24}\text{Na}/^{12}\text{C}(p,pn)^{11}\text{C}$ ratio. (The value was found to be identical within error to the published ratio.¹³) Two measurements involved Al-Cu target stacks for other experiments.¹⁸ When either CH_2 or Cu foils were present, they were downstream of the Al.

In addition to the above, a number of auxiliary experiments were performed. In these, target thickness was substantially increased, or extra mass was added at the window position. These data were used to evaluate the corrections for internal or external secondaries, as will be described below.

The duration of a standard irradiation was 100 beam pulses (~160 sec) at intensities from $\sim 3-9 \times 10^{12}$ protons/pulse. Early experiments which used high efficiency NaI(Tl) well-detectors for ^{24}Na assay were for only 1-10 pulses. After irradiation, autoradiographs of the targets were taken and circular samples, 4.1 cm in diameter centered on the beam spot, were punched out. Assay of ^{24}Na was usually delayed ~15 hrs to permit decay of most of the ^{11}C and ^{18}F . Periodic assays indicated ~1% of the total ^{24}Na fell outside of the punched spot. Corrections for this loss are described below.

Beam Intensity Measurements

A typical system used to measure beam intensities in the present

work is shown schematically in Fig. 1. The heart of a system is a toroidal transformer fabricated from high permeability magnetic tape¹⁹, 25 μm in thickness. The inside diameter of the core is 12.7 cm. Its width is 1.3 cm and the total tape thickness is also 1.3 cm. Passage of the beam bunches through the bore of the transformer induces a signal across the 100 turn secondary winding which, for an open circuit, would be proportional to time rate of change of the beam current. In addition to the signal winding, the transformer has a single turn winding for use in calibrations. Connections between a transformer and its associated electronics, which were located outside the beam tunnel, were via RG-8 or the corresponding solid shielded coaxial cable in areas of severe noise environment. The isolation transformer shown in Fig. 1 served to decouple the grounds and provided additional low frequency noise rejection.

The combination of transformer inductance (~ 0.1 Henry) and cable termination resistor (91Ω) serves as a passive integrator so that the input to the first amplifier stage is proportional to beam current. This stage provides a second integration in a conventional manner and gives an output proportional to the total charge passing through the core aperture. The shunt capacitor across its input terminals serves to keep the signal band-width within the range of the amplifier. A peak-reader, composed of a comparator and sample-and-hold circuit, maintains the maximum signal until it can be digitized. This use of a

peak reader eliminates the need for a beam-time trigger, which is difficult to obtain due to the nature of the extraction process.

In normal operation, the peak reader output is zeroed by a pulse derived from the AGS predetermined clock well before beam ejection time. Digitization is initiated by another pulse from this clock after the beam has passed. Although the circuit is nominally active for the total time between these two pulses, sensitivity to noise is reduced by the fact that the integrator output has a decay time constant of ~ 200 μsec determined by its RC feedback network and the preceding components. In the absence of beam, peak outputs of 100-200 mv are typical, corresponding to $1-2 \times 10^{11}$ protons/pulse when the system calibration is 1×10^{12} protons/volts. When beam is present and exceeds these levels, by a factor of twenty or more as was the case in the present work, only noise occurring within ~ 200 μsec of beam time can have a significant effect. Provided this noise is not correlated with the beam intensity, it will raise the apparent intercept of the system above the level preset under laboratory conditions. In situ calibrations described below should include this effect.

The circuit used for calibrating the beam transformers and associated circuitry is also shown in Fig. 1. A mercury relay is used to connect a charging supply to a precision capacitor which is in series with the single-turn transformer winding. With this

arrangement, the series capacitor and power supply voltage determine the amount of charge transferred, independent of shunt capacitance. As the routine calibration procedure, frequent measurements were made of a system's output with a precision 1602 pF capacitor charged to 100 and to 500 volts, equivalent to 1 and to 5×10^{12} protons per pulse, respectively. These define the slope and intercept of the overall response curves of the different systems used in the present work. Stabilities of $\pm 1\%$ were observed over periods of time up to two weeks which spanned a given series of measurements. Larger shifts occurred when the circuits were shut down for more extended periods between different series of experiments.

More detailed tests of system performance were made occasionally, also using the calibration pulser. Integral linearity was shown to be better than $\pm 0.25\%$ for outputs up to 9 volts. Some systems exhibited larger deviations above this level, and when beam intensities approached 9×10^{12} protons/pulse, the systems sensitivities were intentionally reduced (from 1×10^{12} protons/volt to 2×10^{12} protons/volt) to stay within the linear range.

Perhaps the largest single source of uncertainty in beam intensity measurements stems from the fact that the waveforms of calibration and beam pulses are different. The critically damped current pulse (estimated from the RCL parameters) will fully charge the 1602 pF capacitor in less than 0.5 μ sec, while the 12 beam bunches

are spread over a period of ~ 2.4 μsec . To evaluate the effects of these differences, the calibration pulser was used to deliver the same nominal charge (equivalent to 5×10^{12} protons/pulse) from different capacitors. The results of one such test are shown in Table I. If we consider the results for capacitors from 1602 to 6408 pF, there is no evidence for a dependence of response on capacitor size (or what is equivalent pulse length). The four entries are consistent with a mean value of 0.991 ± 0.005 and imply that the standard deviation of a single value is 0.9 %. This deviation is twice that estimated from different calibrations of the capacitors and the power supplies. A 5% decrease in response is observed with the large, 16022-pF capacitor. It was expected that the circuitry would not perform well with a low amplitude pulse of long duration, and this appears to be the case. Actually, most of the systems used in the present experiment performed better than the illustrative case, e.g., the integrator system used for the 0.8- and 28-GeV measurements at U-167 showed a decrease of only 2% between the 1602 and 16022 pF capacitors. We estimate the waveform dependence might cause an underestimation of beam charge of about 1% which we will include in our systematic errors.

One or more of three transformer and integrator systems were used to measure proton fluences for those activations performed in air at U-801. One transformer, UX801 was located in air at distances of from

4 to 61 cm downstream of the window. A second, UX772, was in vacuum 8.5 m upstream of the window. In the case of the third, UX799 located 27 cm before the window, the aluminum beam pipe passed through the bore of the transformer which was insulated from it. A nearby dielectric break in the vacuum chamber was intended to suppress image currents in the pipe. A single transformer, UX167, was used to monitor the five irradiations at 28 GeV and the three at 0.8 GeV which were performed in the U-167 instrument box.

It was observed in auxiliary experiments that adding mass ahead of a transformer decreased its response. Because this was true both for a transformer in air (UX801) and for one in vacuum (UX167) the effect is not related to air ionization but rather is due to beam interactions which remove positive or add negative particles to the beam. The effect for the 105-mg/cm² window decreased from 0.6% when UX801 was close to the window to 0.3% when it was far removed. After such corrections were applied the beam intensities observed with UX772 and UX801 agreed to within 1%. At the start of the present experiment, the output from UX799 was also in agreement with these two, but it became increasingly erratic and could not be used in later experiments.

Assay of ²⁴Na

The ²⁴Na activities induced in the Al foils of the present work

were determined by assaying the intensity of the 1368-keV γ ray with Ge(Li) detectors in two geometries, at nominal 5- and 10-cm distances from the cryostat face. These devices were calibrated several times during the experiment with standard ^{60}Co sources. As described below, an extrapolation procedure was used to correct for the 36-keV energy difference between the 1332-keV line of ^{60}Co and that of ^{24}Na . In mounting the standards and ^{24}Na samples on Al counting cards, care was taken to maintain constant sample-to-detector distance. Samples were always covered with sufficient Cu to absorb beta particles. 4096-channel γ -ray spectra were recorded at a gain of 0.75 keV/channel and stored on magnetic tape. These were subsequently analyzed to give net counting rates of the 1368- and 2754-keV lines of ^{24}Na and of the 1173- and 1332-keV γ rays of ^{60}Co . Corrections for analyzer deadtime and pileup were made on the basis of a 6-Hz pulser which had been introduced into the counting system at the preamplifier input. No deviations of the decay of ^{24}Na from the expected 15.0-hr half life were observed. A 5.26-y half life was assumed for ^{60}Co .

While such a comparison procedure for ^{24}Na assay is, strictly speaking, not absolute, it has the advantage that ^{60}Co standards are routinely available. Eight different ^{60}Co standards used during the present experiment are identified in Table II. Those denoted NBS-A to E are mixed radiation sources (SRM-4216) containing ^{60}Co which were issued by the National Bureau of Standards yearly starting in 1973.

Their reported uncertainty is 1.4%. Sources IAEA-60 and 99, pure ^{60}Co calibrated by the International Atomic Energy Agency, have a stated accuracy of 0.6%. The remaining standard, JBC-3, was calibrated by comparison with several other standards at BNL, some of which had been calibrated by γ - γ coincidence counting. The entries for each standard in the body of Table II represent a composite of the counting rates observed in the 1173 and 1332-keV lines at the 5 and 10 cm distances divided by the quoted sample disintegration rates and the appropriate mean efficiencies for the lines. In the ideal case, all entries would be unity. The observed deviations reflect differences of one standard from another and/or systematic errors in the counting procedures, e.g., rate dependent effects. The observed counting rates varied over a factor of ~ 150 from NBS-A, the least intense, to IAEA-60 the most intense. Spectra of the mixed standards NBS-D and NBS-E had an appreciable Compton continuum from the 1836-keV γ -ray of ^{88}Y under the 1173 and 1332-keV lines which tests resolution of peak areas from spectra under conditions similar to those expected for ^{24}Na . That all entries in Table II fall so close to unity is strong evidence of the accuracy of the standards and the precision of the Ge(Li) counting procedure.

In order to transfer the calibration from the 1332-keV line of ^{60}Co to 1368 keV, the mean efficiencies measured for the 1173- and 1332-keV lines were first corrected for coincidence summing based on

total efficiency curves for the detectors. Sum corrections varied from 2.1% for 1173 keV to 1.7% at 2754 keV for Ge-13 in the 5 cm geometry. They were proportionally smaller for the less efficient Ge-15 and at the 10 cm distance. Based on the assumption that the peak efficiencies followed a power law dependence on energy, a reduction of 2.6% was inferred for the 36 keV difference.²⁰ The practical efficiency for detecting ^{24}Na was obtained by correcting the extrapolated peak efficiency at 1368 keV for losses due to summing with the 2754-keV gamma. The first detector, Ge-13, calibrated in this way failed after a few experiments and a second one, Ge-15 was used subsequently. Results of three calibrations of Ge-15 are shown in Table III for the two geometries. The good stability shown here when combined with the reproducibility of the ^{60}Co standards evidenced in Table II indicates ^{24}Na can be assayed with an accuracy of better than 1% by this technique.

Since the ^{60}Co standards were point sources, the ^{24}Na efficiencies derived from them are for point sources also. In the present work, corrections for the extended ^{24}Na sources were made on the basis of measured efficiency decreases with lateral displacement of a ^{60}Co point source combined with ^{24}Na activity distributions estimated from autoradiographs of the samples. In the worst cases, the 0.8-GeV experiments where the beam spot was larger than at 28 GeV and at the 5 cm distance, the maximum correction was only 1.9%.

Some early ^{24}Na activity measurements in the present series of experiments utilized the same two well-type NaI(Tl) scintillation detectors which had been used for much earlier studies of the spallation of Al by high-energy protons.^{13,21} The efficiencies of these devices for ^{24}Na had been determined at that time by β - γ coincidence and 4π -counting methods. Since then, these well counters had been used routinely for a variety of beam intensity and diagnostic measurements by foil activation techniques. It could be concluded from the counting rates of ^{137}Cs standards that their efficiencies had remained constant to $\pm 1\%$ over a 15 year period. This was confirmed by intercomparing them with the calibrated Ge(Li) detectors using ^{24}Na either prepared at the AGS or via the $^{27}\text{Al}(n,\alpha)^{24}\text{Na}$ reaction at the BNL cyclotron.

Results and Discussion

A raw cross section for each experiment was calculated from the mean ^{24}Na disintegration rate extrapolated to the midpoint of the irradiation and the proton fluence determined by the current transformers. A correction of from 0.2 to 1.2% was then applied to account for beam particles in the halo which missed the punched area but still passed through the 10 cm aperture of the beam transport system. This correction was based on assays of ^{22}Na inside and outside of the punched circles. The beam halo appeared to be more

intense when determined directly by ^{24}Na . However, auxiliary experiments in which extra mass was present in the target vicinity indicated that about half of the out-of-beam ^{24}Na arose from secondary particles, probably neutrons, rather than true beam protons. Such secondary particles also produce ^{24}Na in the punched foil itself. From several experiments with more massive targets it was concluded that the correction for internally generated secondary particles in our standard 30-mg/cm^2 targets was 0.9% at 28 GeV and 0.4% at 0.81 GeV. The corrections for external secondary particles, i.e. those generated in the 105-mg/cm^2 Al window, was determined in other experiments where extra mass was added at the window position. It was concluded that the window effect decreased from a maximum of 1.2% when foils were close to it, to a negligible value when they were 33 cm downstream. For those irradiations in vacuum at U-167, the effect is absent. Out of beam measurements at U-801 ruled out any contribution of secondaries backstreaming from the meson production target.

The final result of the present work is then a set of 32 values of the $^{27}\text{Al}(p,3pn)^{24}\text{Na}$ cross section at 28 GeV which is presented in the form of a histogram in Fig. 2. The highest and lowest observed values are 8.12 and 7.76 mb respectively, a total range of only 4.5%. The unweighted mean is 7.92 ± 0.02 mb and the standard deviation (s.d.) of a single measurement is 1.3%. Only a small part of this s.d. can be ascribed to true statistical effects, i.e., sufficient

^{24}Na counts were accumulated to give each experiment a precision of 0.5% or better. Although the s.d. observed for subsets composed of measurements performed under nearly identical conditions over a one or two day period did approach the statistical estimate, means of subsets at wider time intervals, or under different conditions typically showed $\pm 1\%$ variability. As one example, two experiments involved simultaneous irradiations of foils at U-167 and U-801 with independent fluences measurements by UX167 and UX801. These gave cross sections of 7.81 and 7.85 mb at U-167 and 8.02 and 7.97 mb at U-801. Another example is the comparison in Fig. 2 of the distribution of the five measurements at U-167 with the complete set. The mean of the five is 7.85 ± 0.02 mb, 1% lower than the overall mean. That the complete set is approximately a Gaussian reflects the variety of experimental conditions employed over the three year period of the present experiment. It is clear that the uncertainty associated with the mean cross section is larger than the observed standard error of the mean, ± 0.02 mb. From a variety of considerations we assign a 1% systematic error to the counting procedure and a 2% systematic error in beam monitoring and arrive at a final value of 7.92 ± 0.18 mb for the $^{27}\text{Al}(p,3p\text{n})^{24}\text{Na}$ cross section at 28 GeV. While this is within errors of the indirectly determined value 8.34 ± 0.45 mb, it is appreciably lower than the 8.6 ± 0.6 mb which had been recommended for use at this energy. The change is in the direction to raise extraction

efficiencies measured by foil activation techniques at the AGS and give better agreement with those obtained by other methods.

Three measurements, performed at U-167 at a beam energy of 0.81 GeV, gave cross sections of 10.92, 10.93 and 10.98. The mean value, $10.94 \pm 0.24 \text{ mb}^{22}$ is in good agreement with the $11.0 \pm 0.5 \text{ mb}$ cross section at 0.59 GeV²³ and with the indirectly determined (via the $^{12}\text{C}(p,pn)^{11}\text{C}$ cross section² and the ratio²¹) value of $10.8 \pm 0.6 \text{ mb}$ at 1.0 GeV.

The absolute $^{12}\text{C}(p,pn)^{11}\text{C}$ cross section at 0.8 GeV has been measured⁶ to be $32.0 \pm 1.0 \text{ mb}$ in an experiment in which proton fluences were determined with an ion chamber whose calibration had been checked against a Faraday cup.⁷ A value of $30.0 \pm 1.1 \text{ mb}$ is inferred from the present $^{27}\text{Al}(p,3pn)^{24}\text{Na}$ cross section and the ratio, 0.365 ± 0.010 .²¹ The 2.0 mb difference is only slightly larger than that expected on the basis of the estimated accuracies of each experiment.

Acknowledgments

The authors are grateful to L. W. Smith of BNL and G. Munday of CERN for their continued support and encouragement. J. Guthy was responsible for the original design of the current integrators. Before they reached the present configuration, the circuits were modified by D. C. Rahm who played an important role in initiating this experiment. We wish to thank J. Curtis for significant contributions during the last measurements. Finally, the experiment would not have been possible without the enthusiastic cooperation of the AGS supporting and operating staffs. This research was carried out at Brookhaven National Laboratory under contract with the U. S. Department of Energy.

References

1. J. B. Cumming, *Ann. Rev. Nucl. Sci.* 13, 261 (1963). This work reviews results from earlier experiments.
2. A. M. Poskanzer, L. P. Remsberg, S. Katcoff, and J. B. Cumming, *Phys. Rev.* 133B, 1507 (1964).
3. B. I. Bekker, V. S. Pantuev, V. A. Sviridov, and M. N. Khachatryan, *Soviet Physics (JETP)* 18, 832 (1964).
4. G. W. Butler, S. B. Kaufman, E. P. Steinberg, and B. D. Wilkins, *Phys. Rev. C* 6, 1153 (1972).
5. S. B. Kaufman, M. W. Weisfield, B. D. Wilkins, D. Henderson, and E. P. Steinberg, *Phys. Rev. C* 13, 253 (1976).
6. K. R. Hogstrom, *Phys. Rev. C* 14, 753 (1976).
7. R. J. Barrett, B. D. Anderson, H. B. Willard, A. N. Anderson, and N. Jarmie, Los Alamos Document LA-6008-MS, unpublished (1975).
8. H. Fuchs and K. H. Lindenberger, *Nucl. Inst. Meth.* 7, 219 (1960).
9. J. B. Cumming, A. M. Poskanzer, and J. Hudis, *Phys. Rev. Lett.* 6, 484 (1961).
10. V. Agoritsas and R. Witkover, *IEEE Trans. Nucl. Sci.* NS-26, 3355 (1979).
11. V. Agoritsas, Y. Y. Lee, and R. Witkover, BNL/AGS Division Tech. Note No. 130 (1977), unpublished.
12. J. B. Cumming, G. Friedlander, and S. Katcoff, *Phys. Rev.* 125, 2078 (1962).
13. J. B. Cumming, G. Friedlander, J. Hudis, and A. M. Poskanzer, *Phys. Rev.* 127, 950 (1962).

14. L. Blumberg, G. Bagley, G. Bennett, J. Claus, J. Curtiss, R. Frankel, H. Hsieh, J. Keane, G. Levine, L. Repeta, J. Schuckman, and A. Soukas, Proceeding of the IXth International Conference on High Energy Accelerators, Stanford (1974) p. 462.
15. W. T. Weng, L. N. Blumberg, E. Gill, A. Soukas, R. L. Witkover, E. Egleman, J. LoSecco, and A. Solak, IEEE Trans. Nucl. Sci. NS-26, 3224 (1979).
16. In this notation, the number gives the approximate distance of the location from the ejection section in feet.
17. A. M. Pokanzer, J. B. Cumming, and R. Wolfgang, Phys. Rev. 129, 374 (1963).
18. J. B. Cumming, R. W. Stoenner, and P. E. Haustein, Phys. Rev. C 14, 1554 (1976).
19. Type 4-79 Mo Permalloy, manufactured by Arnold Engineering Co, Marengo, Illinois.
20. As a check on the extrapolation using the ^{60}Co data, a reverse extrapolation based on the 1368 and 2754-keV lines of ^{24}Na was used. This gave a 3.0% change for the 36 keV difference between 1368 and 1332 keV. Because the pair production process is important at the higher energy and escape peaks subtract from the full energy peak at 2754 keV, it was expected that a larger difference would be observed.
21. J. B. Cumming, J. Hudis, A. M. Poskanzer, and S. Kaufman, Phys. Rev. 128, 2392 (1962).

22. The error includes the same systematic uncertainties as were assumed at 28 GeV.
23. K. Goebel, D. Harting, J. C. Kluyver, A. Kusumegi, and H. H. Schultes, Nucl. Phys. 24, 28 (1961).

Table I. Relative response of a transformer and integrator system to charge equivalent to 5×10^{12} protons as a function of discharging capacitance.

<u>Capacitance(pF)</u>	<u>Relative Output</u>
1602	1.000
3204	0.981
4806	0.997
6408	0.985
16022	0.948

Table II. Intercomparison of various ^{60}Co standard sources using Ge(Li) detectors

Standard/Date	Counting Rate/Disintegration Rate ^a			
	May 1975 ^b	Nov. 1976 ^c	Oct. 1977 ^c	April 1978 ^c
NBS-A	0.999	0.995	0.994	0.996
B	1.003	1.002	0.996	1.003
C	--	0.991	0.999	0.998
D	--	0.998	1.009	1.006
E	--	--	--	0.999
IAEA-60	0.984	1.000	0.998	--
99	1.004	1.016	1.007	1.000
JBC-3	1.010	0.999	0.996	1.000

- (a) The scale for each series of measurements has been normalized so that the average for that series is unity.
- (b) Detector Ge-13, FWHM 1.9 keV at 1332 keV, nominal 10.1% efficiency compared to a 7.6 x 7.6-cm NaI(Tl) scintillator at 25 cm.
- (c) Detector Ge-15, FWHM 1.6 keV at 1332 keV, nominal 8.3% efficiency compared to 7.6 x 7.6-cm NaI(Tl) scintillator at 25 cm.

Table III. Temporal stability of a Ge(Li) detector for detecting the 1368-keV γ ray of ^{24}Na

Date/Source Distance	Absolute Efficiency ($\times 10^4$)	
	5 cm	10 cm
November 1976	14.30	4.94
October 1977	14.47	4.90
April 1978	14.44	4.91
Mean	14.40	4.92
Standard Deviation	0.4%	0.2%

Figure Captions:

Fig. 1. Schematic diagram of a current transformer and its associate readout and calibration electronics.

Fig. 2. Frequency distribution of 28-GeV cross section measurements. The open histogram includes all 32 experimental values. The curve is a Gaussian having the same mean and standard deviation. The cross hatched histogram is the subset composed of the 5 experiments in which the targets were irradiated in vacuum.

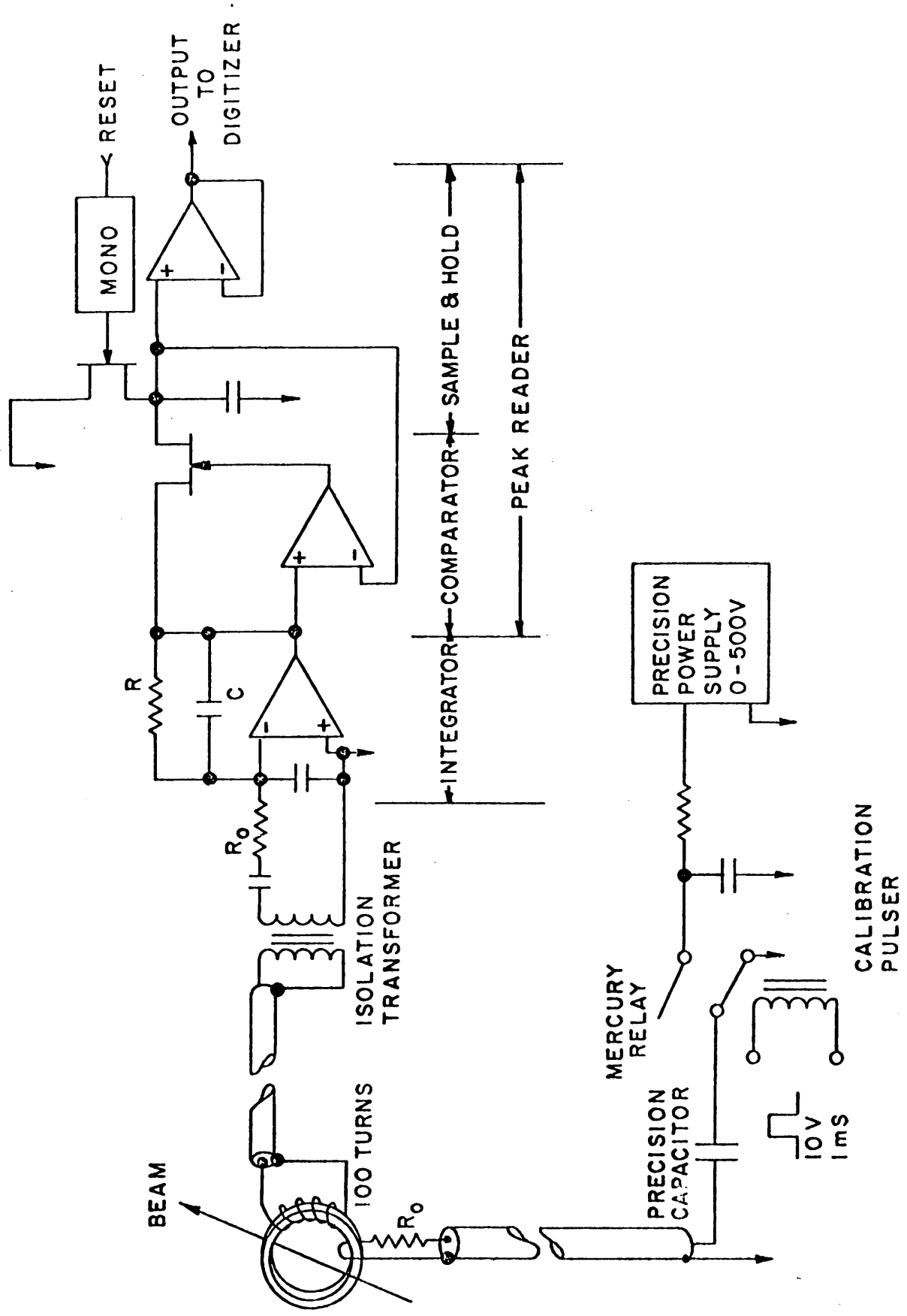


Fig. 1

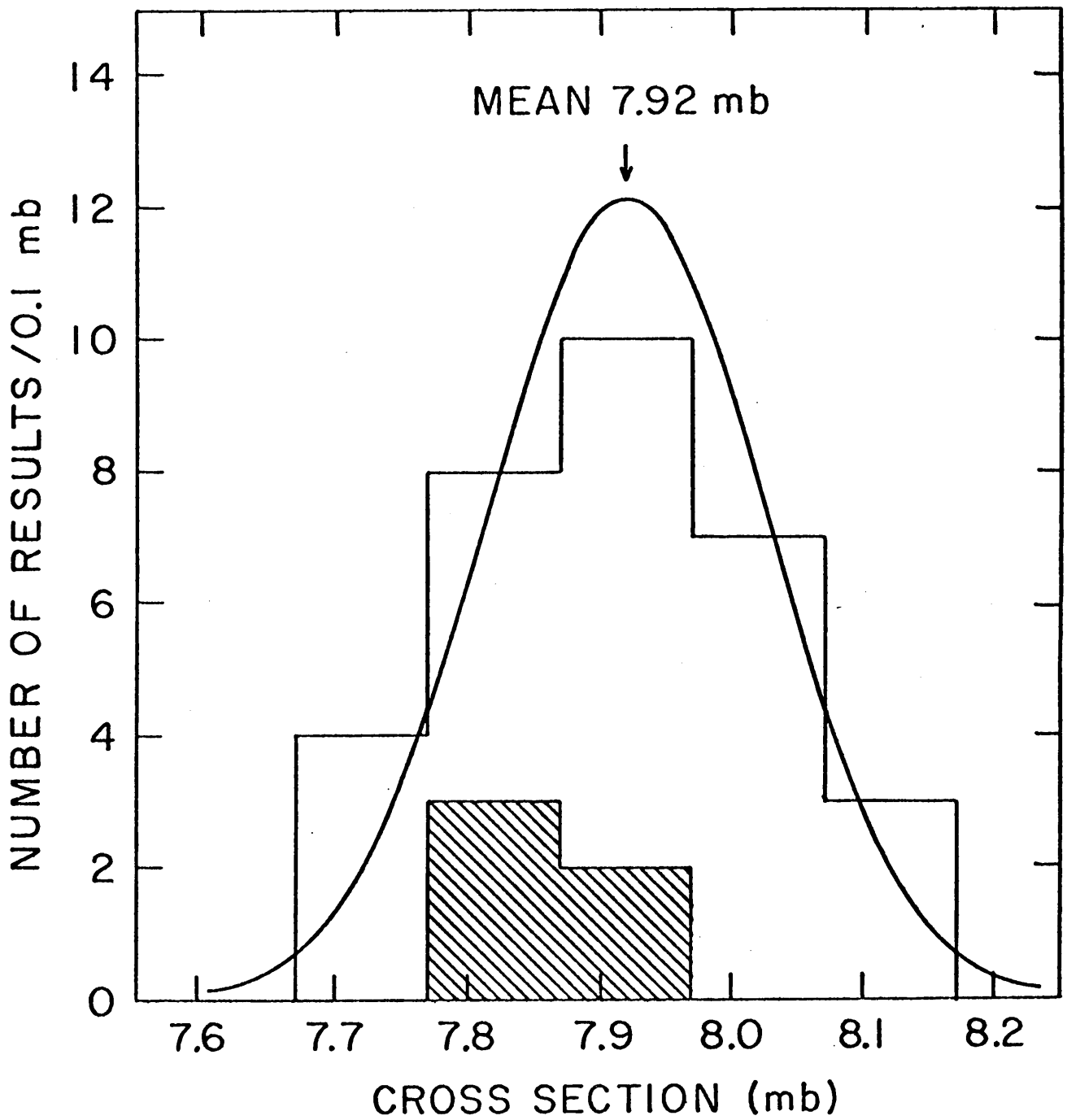


Fig. 2